Repolarization Variability Mechanism and its Relation with Cardiac Arrhythmogenesis

JF Rodriguez[1,3], R Sassi[2], E Pueyo[3,1], L Mainardi[4]

[1]Aragon Institute of Engineering Research, University of Zaragoza, Spain
[2]Dipartimento di Informatica, Università degli Studi di Milano, Italy
[3]CIBER de Bioingeniería, Biomateriales y Nanomedicina (CIBER-BBN), Zaragoza, Spain
[4]Dipartimento di Bioingegneria, Politecnico di Milano, Italy

Abstract

Enhanced temporal variability of ventricular repolarization has been related to increased ventricular arrhythmic risk. In this study, we investigate the influence of stochastic ion channel gating on the variability of four arrhythmic risk biomarkers: action potential (AP) duration (APD), AP triangulation and systolic and diastolic calcium levels. Different levels of white noise, representing different channel numbers, were introduced by means of a stochastic differential equation for the gating variables of the ten Tusscher-Panfilov human ventricular model (TP06). In single cells the rapid and slow delayed rectifier potassium currents (I_{Kr} and I_{Ks}) were the main contributors to biomarkers variability, which was shown to be increased at fast pacing frequencies, particularly for APD and diastolic calcium. At tissue level, electrotonic coupling masked the effects of stochastic gating on the variability of all the investigated biomarkers. In particular, a very notable reduction in variability was obtained for 2D and 3D tissue models, with 80% reduction with respect to 1D models, and more than 20 folds with respect to isolated cells under physiological conditions. This indicates that large variations in cellular AP are required in order to reproduce physiological variability levels measured in tissue.

1. Introduction

Beat-to-beat repolarization variability (BRV) is an intrinsic characteristic of cardiac function that is evidenced at different scales, from temporal variations in the action potential (AP) duration (APD) of the isolated cardiomyocyte [1] to QT variability at the body surface [2]. A number of studies have linked enhancement in temporal variability of cardiac repolarization to an increased risk of developing arrhythmias [2, 3]. In addition, under pathologic conditions, beat-to-beat variability has been identified as a better proarrhythmic marker than QT prolongation [2].

A number of studies have proposed stochastic ion-channel gating as a source of variability in ventricular repolarization [4, 5]. These studies have introduced stochastic gating in one or several ionic currents and have investigated their effects on APD variability. In this study we introduce stochastic ion-channel gating in four ionic currents of the ten Tusscher-Panfilov (TP06) human ventricular AP model [6] that have been identified to significantly influence BRV [1], namely, I_{Ks}, I_{Kr}, I_{CaL}, and I_{to}. The effect of current fluctuations is evaluated on four different arrhythmic risk biomarkers: systolic and diastolic $[Ca^{2+}]_i$, APD_{90} and AP triangulation (APD_{90}-APD_{50}), when stimulating at different pacing frequencies. In addition, the influence of electronic coupling on APD variability is investigated in one-, two- and three-dimensional (1D, 2D, 3D) tissues. Unless otherwise stated, APD is used to refer to APD measured at 90% repolarization (APD_{90}).

2. Methods

2.1. Stochastic gating

Stochastic gating at the ionic level was introduced by replacing the Hodking-Huxley formulation for the current gating variable by a formulation based on the Langevin equation [5, 7] given by the following stochastic differential equation (SDE):

$$dg = \frac{g_\infty - g}{\tau_g}dt + \sqrt{\frac{g_\infty + (1-2g_\infty)g}{N\tau_g}}dW, \quad (1)$$

where g_∞ and τ_g are the steady-state value of g and the time constant to reach that steady-state value, W represents a Wiener process, and $N > 0$ is a parameter controlling the magnitude of the noise introduced. We associated N to the number of channels expressed in the membrane.

Stochastic gating in the TP06 model was incorporated in nine gates related to the ionic currents considered. Namely,

i) I_{Ks} current, the activation gate x_s; ii) I_{CaL} current, the activation gate d, the slow inactivation gate f, the fast inactivation gate f_2, and the calcium inactivation gate f_{cass}; iii) I_{to} current, the activation r, and inactivation s, gates; iv) I_{Kr} current, the activation x_{r1}, and inactivation x_{r2}, gates.

The number of channels in the cell membrane for each of the considered currents required in Eq.1 were obtained from the literature and are given in Table 1.

Table 1. *Average number of channels used for the simulations.*

Current	N	Ref
I_{Ks}	12000	[5]
I_{CaL}	50000	[8]
I_{Kr}	2175	[9]
I_{to}	1495	[10]

2.2. Stimulation protocols and biomarkers of arrhythmic risk

Two stimulation protocols were applied and four cellular biomarkers of arrhythmic risk were computed:

Steady-state protocol. The model was stimulated for 60 min at a frequency of 1Hz. APD_{90}, AP triangulation and systolic and diastolic $[Ca^{2+}]_i$ levels were recorded for the last minute of stimulation.

Dynamic restitution protocol. After reaching steady state, the model was stimulated for 5 min at increasing frequencies from 1Hz up to 5Hz, recording the last minute of stimulation. Rate dependent curves for all biomarkers were obtained.

2.3. Numerical implementation and simulation

Model differential equations were implemented in C. Cells were stimulated with square transmembrane current pulses with an amplitude -24 pA/pF and 1 ms duration. Forward Euler integration with a time step of 0.02 ms was used to integrate the system of differential equations governing the cellular electrical behavior of epicardial cells. The Rush and Larsen integration scheme was used to integrate the Hodgkin-Huxley type equations for the gating variables non subjected to fluctuations, whereas SDEs were integrated using the Euler-Maruyama method.

A monodomain reaction-diffusion equation was used to model the electric propagation across the cardiac tissue. This partial differential equation (PDE) was solved using the finite element method with linear interpolation functions, a time step of 0.02 ms and spatial discretization of 0.01 cm by means of the software ELVIRA [11, 12]. The different tissue models were paced at 1Hz for 6 minutes. The last minute of activity was used for variability computation.

2.4. Statistics

The mean and standard deviation (SD) of each biomarker were computed based on five realizations consisting on records one minute long each. Variability is reported as the Coefficient of Variation (CV) in percentage, defined as CV=100×SD/mean.

3. Results

3.1. Effect of stochastic channel gating on BRV and model stability

The suitability of modeling multi-channel stochastic behavior using a Langevin SDE was checked by observing the long term model response under stochastic channel gating. After 60 minutes of stimulation at 1 Hz, the differences in the intracellular potassium $[K^+]_i$, among the deterministic and stochastic models was less than 0.01% along a beat (Figure 1a). Similar results were obtained for $[Na^+]_i$ and $[Ca^{2+}]_i$ concentrations. In addition, Poincaré plots of APD_{i+1} versus APD_i show the same temporal dynamics, circular shape (Figure 1b) as observed in experiments [1, 13].

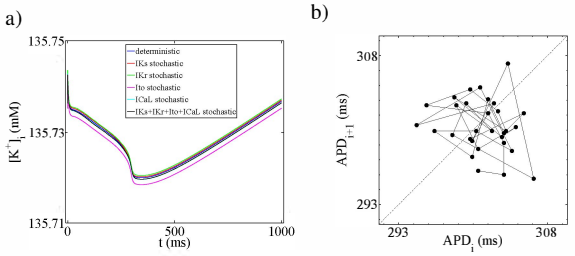

Figure 1. *Long term response of TP06 model with stochastic channel gating. a) Intracellular potassium concentration after 60 min of stimulation at a cycle length (CL) of* 1000 *ms for the deterministic and stochastic models; b) Poincaré plot of 60 consecutive APDs at CL=*1000 *ms in the model with stochasticity in all currents.*

3.2. Effect of stochastic channel gating on biomarkers

Stochastic gating did not affect the rate dependence of the average value for the four biomarkers with respect to the deterministic model (Figure 2). However, fluctuations of the main repolarization currents, i.e., I_{Kr}, and I_{Ks}, led to early appearance of alternants in the model, preventing complete repolarization for CLs below 250 ms (see Figure 2).

Fluctuations in I_{Ks} were found to be the main contributor to BRV for all biomarkers (Figure 3), with exception to the

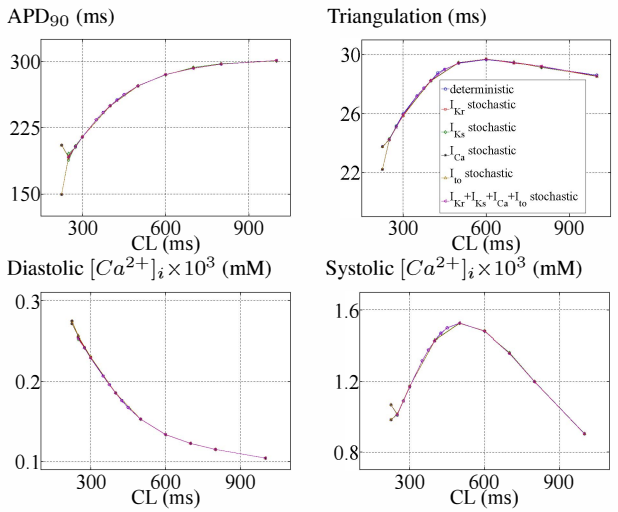

Figure 2. *Rate dependence for the four biomarkers in the TP06 model.*

triangulation where fluctuations in I_{Kr} were more significant (Figure 3b). We also found that the variability computed when the four currents were made stochastic did not correspond to the sum of the individual contributions, as observed in [4].

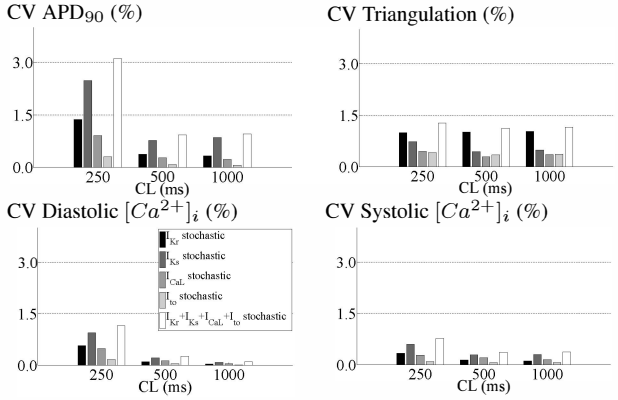

Figure 3. *CV for the four biomarkers in the TP06 model for three CLs: 250, 500, and 1000 ms.*

Figure 3 also shows that CV increases with the pacing frequency for APD and diastolic $[Ca^{2+}]_i$ biomarkers, whereas for triangulation and systolic $[Ca^{2+}]_i$ biomarkers the CV remained almost constant along the tested frequencies. A more detailed observation of the evolution of the CV and SD of the APD for different CLs indicates that CV slightly increases for frequencies up to 2.8 Hz whereas the SD decreases, also slightly (see Figure 4). However, as the stimulation frequency increases above 2.8 Hz, both the CV and SD show a consistent increment. This behavior is also observed for diastolic $[Ca^{2+}]_i$ (not shown), whereas for the triangulation and systolic $[Ca^{2+}]_i$ no significant changes in variability were observed in the range of CLs studied.

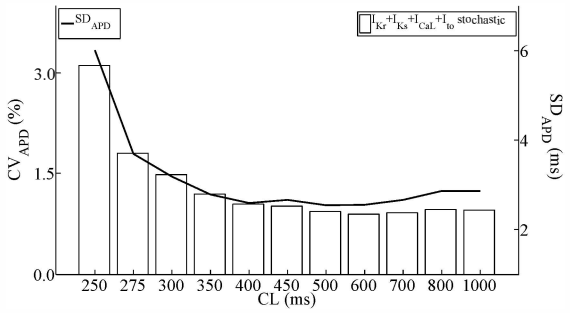

Figure 4. *CV (bar plot) and SD (solid trace) for the APD_{90}.*

3.3. Effect of electronic interaction

As demonstrated in previous studies, electrotonic interaction reduces the variability observed in tissue [1, 4, 5]. However, these studies have focused mostly on one-dimensional tissue models. We considered 1D (4 cm cable), 2D (0.5×2 cm^2 rectangle), and 3D ($0.08\times0.08\times1.25$ cm^3 slab) tissue models in which the maximum propagating velocity was set to 68 cm/s [6], with a transverse to longitudinal velocity ratio of 0.57. The tissue was considered as homogeneous (composed of epicardial cells only) and transversally isotropic, with the fiber direction coinciding with the largest dimension of the geometry. For simplicity only fluctuations in I_{Ks} were considered for the tissue simulations.

Table 2. *CV for the APD in 1D, 2D, and 3D tissue models stimulated at 1Hz, with variability induced by fluctuations in the I_{Ks} current.*

Model Dim	N_{Ks}	CV (%)	N_{Ks}	CV (%)
Unicell	12000	0.85±0.08	75	10.87±1.01
1D	12000	0.082±0.006	75	0.946±0.066
2D	12000	0.031±0.004	75	0.209±0.030
3D	12000	0.031±0.001	75	0.175±0.026

Table 2 (second column) shows the CV of APD for the different tissue models as well as for the isolated cell. The table shows that for the number of I_{Ks} channels given in Table 1, electronic coupling results in 90% reduction in APD variability over 60 consecutive cardiac cycles at 1Hz pacing in the 1D tissue (same as obtained in [5]). On the contrary, this reduction in APD variability reaches 96% in 2D and 3D tissues. Therefore, dimensionality significantly affects APD fluctuations. Even though results for isolated cells are in good agreement with experimental results in

isolated cells [5], the results obtained in the 3D tissue are clearly underestimated with respect to the variability measured in papillary muscles [5]. In order to reach this degree of variability in the numerical model, the fluctuations at cellular level must be increased to values shown in Table 2 (third column). In fact, for this setting, the variability obtained in the 1D and 3D tissues models are much closer to those reported by Zaniboni et al. for coupled cells (1.5%) of guinea pig, and by Pueyo et al. in human papillary muscle (0.44%). In addition, the large fluctuations introduced in the model did not affect the stability of the model (results not shown). In this regard, the isolated cell showed similar restitution curves for the deterministic and stochastic models for CLs down to 250 ms, with fluctuations preventing complete repolarization for CLs below 250 ms.

4. Discussion and conclusions

We have used a Langevin SDE to introduce stochastic fluctuations in the main repolarization and plateau currents of the TP06 human AP model, studying the effect on four different biomarkers of arrhythmic risk. Our results indicate that fluctuations on I_{Ks} have the largest contribution to BRV, in agreement with previous observations [4, 5, 13]. In addition, our simulations indicate a non-monotonic dependence of APD and diastolic $[Ca^{2+}]_i$ variability with CL. In this regard, variability decreases (slightly) with the CL up to a CL close to 400 ms. For lower cycle lengths, the APD variability starts to increase until the appearance of alternants due to incomplete depolarization of the cell. This implies that fluctuations may reduce the effective refractory period of the tissue, increasing its vulnerability to conduction block. In addition, the increments in APD variability occur for low CLs, which corresponds to the region of higher arrhythmic risks in tissue. Therefore, it is possible that BRV plays an important role in triggering and modulating the arrhythmic behavior in cardiac tissue.

We have observed that problem dimensionality affects the reduction in APD variability. The large difference observed in Table 2 between 1D and 2D/3D tissues is related to the larger component of the axial current present in the higher dimensional problems. In 1D, the axial current has only components along the cable, whereas in two and three dimensions the axial current has multi-dimensional contributions. This makes the 2D and 3D problems more diffusive, which contributes to reduce the fluctuations found at cell level. This implies that in order to reproduce experimental observations of variability in tissue, the fluctuations at cell level must be increased to values at least four times larger than those reported in isolated-cell experiments.

Acknowledgements

This work was supported by projects TIN2012-37546-C03-03 and TEC2010-19410 from Spanish Ministry of Economy and Competitiveness (MINECO), Spain. E.P. acknowledges the financial support of Ramón y Cajal program from MINECO.

References

[1] Zaniboni M, Pollard A, Yang L, Spitzer K. Beat-to-beat repolarization variability in ventricular myocytes and its suppression by electrical coupling. Am J Physiol Heart C 2000; 278(3):H677–H687.

[2] Hinterseer M, Beckmann BM, Thomsen MB, Pfeufer A, Ulbrich M, Sinner MF, et al. Usefulness of short-term variability of QT intervals as a predictor for electrical remodeling and pro arrhythmia in patients with nonischemic heart failure. Am J Cardiol 2010;106:216–220.

[3] Myles RC, Burton FL, Cobbe SM, Smith GL. The link between repolarization alternans and ventricular arrhythmia: does the cellular phenomenon extend to the clinical problem? J Moll Cell Cardiol 2008;45:1–10.

[4] Lemay M, de Lange E, Kucera J. Effects of stochastic channel gating and distribution on the cardiac action potential. J Theor Biol 2011;281(1):84–96.

[5] Pueyo E, Corrias A, Virág L, Jost N, Szél T, Varró A, et al. A multiscale investigation of repolarization variability and its role in cardiac arrhythmogenesis. Biophys J 2011; 101(12):2892–2902.

[6] ten Tusscher K, Panfilov A. Alternans and spiral breakup in a human ventricular tissue model. Am J Physiol Heart C 2006;291(3):1088–1100.

[7] Van Kampen N. Stochastic processes in physics and chemistry. North-Holland, Amsterdam: Elsevier, 1992.

[8] Greenstein J, Winslow R. An integrative model of the cardiac ventricular myocyte incorporating local control of Ca^{2+} release. Biophys J 2002;83(6):2918–2945.

[9] Veldkamp M, van Ginneken A, Bouman L. Single delay rectifier channels in the membrane of rabbit ventricular myocytes. Circ Res 1993;72:865–878.

[10] Fedida D, Giles W. Regional variations in action potentials and transient outward current in myocites isolated from rabbit left ventricle. J Physiol 1991;442:191–209.

[11] Heidenreich E, Ferrero J, Doblare M, Rodriguez J. Adaptive macro finite elements for the numerical solution of monodomain equations in cardiac electrophysiology. Ann Biomed Eng 2010;38(7):2331–2345.

[12] Niederer SA, Kerfoot E, Benson AP, Bernabeu MO, Bernus O, Bradley C, et al. Verification of cardiac tissue electrophysiology simulators using an n-version benchmark. Philos T Roy Soc A 2011;369(1954):4331–4351.

[13] Heijman J. Computational analysis of beta-adrenergic stimulation and its effects on cardiac ventricular electrophysiology. Maastricht University, 2012.

Address for correspondence:

Jose F. Rodriguez
Mechanical Engineering department / University of Zaragoza
Edf. Betancourt, Maria de Luna S/N / 50018 Zaragoza / Spain
jfrodrig@unizar.es